Biochemistry and Biophysics Reports 7 (2016) 56–62

Contents lists available at ScienceDirect

Biochemistry and Biophysics Reports

journal homepage: www.elsevier.com/locate/bbrep

# Actin exposure upon tissue injury is a targetable wound site-specific protein marker

Erik D. Pendleton [a,1], Challise J. Sullivan [a,1], Henri H. Sasmor [a], Kristy D. Bruse [b], Tifanie B. Mayfield [a], David L. Valente [a], Rachel E. Abrams [a], Richard H. Griffey [a], John Dresios [a,*]

[a] Leidos, Inc., 10260 Campus Point Drive, San Diego, CA 92121, United States
[b] Lovelace Respiratory Research Institute, 2425 Ridgecrest Drive SE, Albuquerque, NM 87108, United States

ARTICLE INFO

*Article history:*
Received 9 November 2015
Received in revised form
5 April 2016
Accepted 17 May 2016
Available online 18 May 2016

*Keywords:*
Injury
Wound
Bleeding
Hemorrhage
Protein marker
Actin

ABSTRACT

*Background:* Identification of wound-specific markers would represent an important step toward damaged tissue detection and targeted delivery of biologically important materials to injured sites. Such delivery could minimize the amount of therapeutic materials that must be administered and limit potential collateral damage on nearby normal tissues. Yet, biological markers that are specific for injured tissue sites remain elusive.
*Methods:* In this study, we have developed an immunohistological approach for identification of protein epitopes specifically exposed in wounded tissue sites.
*Results:* Using *ex-vivo* tissue samples in combination with fluorescently-labeled antibodies we show that actin, an intracellular cytoskeletal protein, is specifically exposed upon injury. The targetability of actin in injured sites has been demonstrated *in vivo* through the specific delivery of anti-actin conjugated particles to the wounded tissue in a lethal rat model of grade IV liver injury.
*Conclusions:* These results illustrate that identification of injury-specific protein markers and their targetability for specific delivery is feasible.
*General significance:* Identification of wound-specific targets has important medical applications as it could enable specific delivery of various products, such as expression vectors, therapeutic drugs, hemostatic materials, tissue healing, or scar prevention agents, to internal sites of penetrating or surgical wounds regardless of origin, geometry or location.


## 1. Introduction

There are a milieu of biochemical and physiological events at a wound site due to structural changes resulting from cell lysis or tissue rupture and the associated displacement of intracellular or extracellular proteins from their natural locations. Studies in model organisms, such as zebrafish, demonstrated that myocellular injury leads to expression of specific markers, such as Xin-actin-binding repeat-containing proteins (Xirp), with a potential role in cytoskeletal reorganization and muscle regeneration [13]. Other studies have shown that injury of the blood vessel wall and surrounding extracellular matrix by mechanical rupture or heat results in irreversible unfolding of collagen from its native state [22], generating signals for induction of arteriolar vasodilation and increase in blood flow to the injured area [10]. In addition, necrotic cells resulting from tissue injury can be detected by the immune system through recognition of damage-associated molecular patterns (DAMPs) by dendritic cell receptors, leading to inflammatory response and tissue repair [2,16]. Identification of targetable wound-specific markers would represent a viable mechanism for the detection and specific delivery of biologically important materials to wound surfaces, such as therapeutic or hemostatic payloads. Additionally, identification of such targets might be advantageous in minimizing administered dosages, improve the availability due to increased local delivery, and avoid potential deleterious interactions with nearby healthy tissue. Wound targeting would also enable binding to non-compressible, asymmetrically exposed internal organ areas as a result of penetrating or surgical wounds, irrespective of geometry and location. To date, however, biological epitopes that are specific to injured tissue sites remain largely unknown.

The objective of this study was to identify protein markers that become rapidly exposed in wounded animal tissues and might be

* Correspondence to: Leidos, Inc., 10260 Campus Point Drive, SanDiego, CA 92121. U.S.A.
*E-mail address:* john.dresios@leidos.com (J. Dresios).
[1] These authors contributed equally to this work.

http://dx.doi.org/10.1016/j.bbrep.2016.05.013

useful for injury site detection and/or targeted delivery of therapeutic products to the trauma surface, irrespective of wound shape and/or location. We hypothesized that rapid site detection and wound-specific delivery of medical products would require recognition of structural, physical and/or biochemical signatures unique to the damaged tissue that are present at the wound site immediately upon injury. To this end, we developed a method for screening and identifying proteins that are rapidly and specifically exposed in injured animal tissues. Using this approach, we identified an abundant cytoskeletal protein as a wound marker and evaluated its targetability for localized delivery of materials at the site of the wound both *ex vivo* and *in vivo*.

## 2. Materials and methods

### 2.1. Reagents

2-(N-morpholino)ethanesulfonic acid (MES) buffer, Bovine serum albumin (BSA) and $NaN_3$ were purchased from Sigma-Aldrich Corporation, MI. Fetal Bovine Serum (FBS) Hyclone, 10% Neutral Buffered Formalin, Tissue Tek optimum cutting temperature (O. C. T.) compound, sucrose, and Fluorescent Mounting Media were purchased from VWR International, PA. Tween-20 10% was purchased from Bio-Rad Laboratories, CA. Carboxylated fluorescent (505/515) 2 μm beads were purchased from Invitrogen, CA. 1-Ethyl-3-(3-dimethylaminopropyl) carbodiimide hydrochloride (EDC) and N-hydroxysulfosuccinimide (Sulfo-NHS) were purchased from Thermo Scientific, IL. DAPI (4′,6-Diamidino-2-Phenylindole, Dihydrochloride) was purchased from Thermo Fisher Scientific, MA.

### 2.2. Antibodies

Anti-β-Actin-Fluorescein isothiocyanate (FITC) mouse monoclonal antibody and mouse IgG1 anti-β-actin were purchased from Sigma-Aldrich Corporation, MI. Alexa-488 donkey anti-mouse IgG and goat anti-mouse IgG1 were purchased from Jackson ImmunoResearch, PA. Anti-collagen I, anti-Elastin, anti-Entactin and mouse IgG1 anti-human IgM were purchased from AbCam, MA. Alexa 488 anti-S6 ribosomal 54D2 antibody was purchased from Cell Signaling Technology, MA.

### 2.3. Antibody fluorescent labeling

Anti-Collagen I, anti-Elastin, anti-Entactin and mouse IgG1 anti-human IgM were FITC-labeled using N-Hydroxysuccinimide (NHS)-Fluorescein (Thermo Fisher Scientific, MA) according to manufacturer's recommendations with slight modifications. Briefly, the antibody sample (1 mg/mL) was mixed with freshly reconstituted NHS-Fluorescein in DMSO and the labeling reaction was incubated overnight (12–16 h) at 4 °C. The labeled antibody was then separated from excess fluorescein reagent utilizing MicroSpin G-25 columns (GE Healthcare Bio-Sciences Corporation, PA) per the manufacturer's recommended conditions. Protein concentration in the eluant was estimated utilizing the Pierce™ BCA Protein assay kit (Thermo Fisher Scientific, MA). The efficiency of antibody fluorescence labeling was measured using a Mithras LB 940 multimode microplate reader (Berthold Technologies, TN). Antibody preparations used in these studies had similar specific fluorescence intensities.

### 2.4. Ex vivo tissue samples

Rat tissues for *ex vivo* experiments were harvested from healthy male Sprague-Dawley rats and immediately snap frozen in liquid nitrogen. Rat liver tissue was purchased from BioChemed Services (Winchester, VA) or Analytical Biological Services, Inc. (Wilmington, DE). Rat kidney and rat spleen tissues were purchased from Innovative Research, Inc. (Novi, MI). Rat skeletal muscle tissue was purchased from BioreclamationIVT (Liverpool, NY). Bovine whole blood with sodium heparin anticoagulant was purchased from Innovative Research, Inc. (Novi, MI).

### 2.5. Tissue injury ex vivo and wound targets screening

The rat tissue samples (approximately $2 \times 2 \times 2\ cm^3$ in size) were thawed at 4 °C and, depending on the type of tissue, dissection scissors, forceps, or razor blades were used to create an X-shaped wound. The wounds covered the majority of the surface area, measuring approximately 1.5 cm in diameter and cutting all the way through the tissue, top to bottom. Immediately following injury, the tissue samples were placed in 5 mL cold blocking solution (10% FBS in PBS) and incubated for 1 h at 4 °C. FITC-labeled antibodies against the potential injury-specific target epitopes (or anti-mouse IgG as negative control) were diluted in blocking solution (500 μL at a final concentration of 0.05 μg/μL) and added to tissue samples followed by incubation at 4 °C for 1 h. After antibody incubation, 1 mL cold PBST (0.1% Tween-20 in PBS) was added to the wound to remove unbound antibody (total of two washes). The samples were fixed by placement in a 35 mL cold 10% Neutral Buffered Formalin (VWR International, PA) followed by overnight fixation at 4 °C. Samples were then placed in 35 mL cold 30% Sucrose/PBS overnight at 4 °C for cryoprotection. The samples were mounted into cryomolds in O.C.T. medium, with the X-shaped wound facing the bottom of the cryomold, and placed in a −70 °C freezer. Frozen blocks were shipped to Molecular Diagnostic Services (CA) for cryosectioning using a microtome to 10-micron thick sections, and mounting of the tissue sections onto microscope slides. For analysis, slides were warmed to room temperature and submerged in PBS for 5 min before applying Fluorescent Mounting Media (VWR International, PA) and coverslips. Tissue slides were viewed using an Olympus IX51 inverted microscope (Olympus, MA). Images were captured using a MicroFire™ digital microscope imaging camera and Picture Frame™ software (Optronics Engineering Ltd., TX). For nuclear staining, tissue sections were incubated with DAPI [(100 ng/mL in phosphate-buffered saline (PBS))] in dark for 5 min at room temperature prior to fluorescence imaging. For testing antibody binding in the presence of blood, wounded tissue samples were immersed in bovine blood and incubated for 1 h with FITC-labeled antibodies (anti-β-actin or IgG) previously diluted in heparinized bovine blood (antibody final concentration 0.05 μg/μL). The rest of the experimental processes were performed essentially as described above.

For quantitative analysis of the specific signal increase within the injury sites relative to uninjured tissue, images from tissues treated with fluorescently labeled antibodies were converted to grayscale and multiple representative rectangular regions were selected from the wounded surface as well as the neighboring healthy tissue (Supplemental Fig. 1). Quantitative analysis was performed as an aggregate for all selected wounded regions. Same analysis was performed for the selected healthy tissue regions to represent the background. The resulting mean values and standard deviations were calculated and graphically represented using Matlab R2013b software (MathWorks, Natick, MA).

### 2.6. Microbead-antibody conjugation

Yellow-green fluorescent carboxylate-modified microspheres (nominal bead diameter of two microns) (Thermo Fisher Scientific, MA) were washed by mixing 500 μL of beads suspension (2%) with

1 mL of 100 mM MES pH 5.0 followed by centrifugation at 5000 × *g* for three minutes. The supernatant was discarded and the beads were re-suspended in 800 μL of the same buffer. Freshly prepared EDC (40 μL, 100 mg/mL) was then added to the beads followed by mixing and addition of freshly prepared sulfo-NHS (160 μL, 50 mg/mL). The mixture was placed in a shaking incubator at 1400 rpm for 15 min at room temperature. Beads were spun down and the supernatant discarded. The beads were re-suspended in 1 mL PBS, pelleted, and re-suspended in one mL solution consisting of equal volumes of PBS and goat anti-mouse IgG1 (1.2 mg/mL) followed by overnight incubation on an orbital shaker at 4 °C. The beads were pelleted by centrifugation at 5000 × *g* for three minutes and re-suspended in one mL of 40 mM glycine solution followed by incubation on an orbital shaker for 30 min at room temperature. The beads were sonicated in a water bath for 30 min and vortexed to disperse any clumps. The beads were then washed in buffer A (PBS, 1% BSA, 0.5% Tween-20) and re-suspended in one mL of sample buffer (PBS, 1% BSA, 0.05% Tween-20, 0.02% NaN3/PBS). Anti-actin or anti-IgG antibody (200 μL, 2 mg/mL) were then added and the solution was mixed on an orbital rocker for 2 h at room temperature, followed by 72 h at 4 °C. At the end of the incubation period, beads were pelleted, washed twice in 500 μL of sample buffer, re-suspended in the same buffer, and stored at 4 °C.

### 2.7. Wound site recognition by antibody-conjugated microbeads

All animal research activities were conducted at the Lovelace Respiratory Research Institute (LRRI) under an Institutional Animal Care and Use Committee (IACUC) approved animal use protocol. Male Sprague-Dawley rats (approximately 300 g) were anesthetized via isoflurane inhalation and subjected to mid-line ventral incision. The large liver lobe was isolated and severe parenchymal hemorrhage was created by laceration of a section of the ventral surface with a curved set of surgical scissors, generating a grade IV open abdomen trauma. Wounds were approximately 1.5 cm × 0.75 cm × 0.4 cm (2.1–5.6% of the total liver weight, as determined post-experimentation; approximate excised tissue volume was 600–700 μL). At five minutes post injury (blood loss was approximately 0.5 mL/min), fluorescently labeled polystyrene beads (500 μL, $2 \times 10^6$ beads/μL in sample buffer), tagged with either anti-actin antibodies (for wound targeting) or anti-IgG (negative control), were applied to the wound over a 30 s period. Ninety seconds after the beads were applied, the animal was euthanized and the liver removed. The injured lobe was separated from the rest of the liver and the wound was washed four times with 1 mL of cold buffer consisting of PBS, 0.1% Tween-20% and 0.02% NaN3/PBS. Liver tissue was then fixed and processed for fluorescence imaging as described previously.

Conjugated microparticle testing *ex vivo* was performed essentially as described above using excised rat liver subjected to X-shaped wound. In these experiments, 200 μL of blocking solution was applied to the wound and incubated for two minutes followed by addition of polystyrene beads (83 μL, $5 \times 10^6$ beads/μL in sample buffer) and incubation for 2 min. The wound was washed four times with PBS, 0.1% Tween-20 solution, and the tissue was fixed, cryo-sectioned, and imaged as described previously.

## 3. Results

### 3.1. Screening against protein epitopes exposed in wounded tissue

The specific injury-induced exposure of candidate protein epitopes was tested in a rat injured liver tissue *ex-vivo*. A schematic description of the experimental process is illustrated in Fig. 1A. In these experiments, animals were euthanized and the tissue was excised from the body and immediately snap frozen. Upon thawing, the tissue was lacerated and incubated with labeled (fluoresceinated) antibodies against the candidate target epitopes or with non-specific IgG antibodies as negative control. Following tissue fixation and cryosectioning, the slides containing tissue samples were examined using fluorescence imaging microscopy for the identification of protein targets that are exposed in injured tissue as a means of their interaction with their cognate labeled antibodies. For a candidate epitope to be identified as a wound target, the signal from the labeled antibody should be localized in the wounded tissue surface rather than the surrounded healthy tissue area and be higher than the signal generated by the incubation of a wounded surface with a negative control antibody.

The list of candidate wound epitope targets included proteins that were expected to be exposed at high concentrations in the wounded area upon cell lysis caused by trauma and also of partially insoluble nature so that they would be able to remain at the injured site despite the potential presence of significant blood flow. Criteria for inclusion of a candidate target epitope to the screening list also included the availability of an antibody against that epitope as well as lack of significant cross reactivity of available antibodies toward other epitopes. As a result, the list of candidate wound epitope targets consisted of intracellular proteins, such as cytoskeletal (actin and myosin), nuclear (histones) and cytosolic (ribosomal) proteins, as well as extracellular matrix proteins, such as collagen I (among the most abundant arterial wall proteins), entactin (a component of the basement membrane), and elastin (a component of the vessel wall).

### 3.2. Identification of actin as a wound-specific target epitope

Antibodies against the aforementioned candidate protein targets were obtained and labeled with fluorescein. The results indicated that anti-β-actin antibody binds to the edges of the wound but not to surrounding healthy tissue of rat liver and that such wound site binding generates a signal that is significantly stronger than the signal observed using labeled control IgG (Fig. 1B and C). In contrast to actin, negligible binding to the injured site was observed using antibodies against other intracellular proteins, such as ribosomal proteins, histone, and myosin, or extracellular matrix proteins, such as collagen I, entactin and elastin (Fig. 1D). Results from the quantitative analysis of the data are shown in Fig. 1E illustrating the stronger binding to wounded areas *versus* nearby healthy tissues of actin antibody relative to other antibodies tested.

After demonstrating that β-actin was exposed in injured rat liver tissue, we tested whether this protein represents an injury recognition target for other tissues as well. The results in Fig. 2 demonstrated that actin is exposed in injured rat spleen, kidney and skeletal muscle tissues, suggesting its broad applicability as an injury-specific epitope. Preliminary assessment of the binding kinetics of actin recognition at the wound area, performed by incubating the antibody with the tissue for different time frames, indicated that wound-specific binding occurs within 30 s (Fig. 3A and B). In addition, the targetability of this protein was not hindered by the presence of blood in the wounded area as shown in experiments where the *ex vivo* wound tissue was immersed in blood prior to the application of the FITC anti-actin antibody (Fig. 3C and D).

### 3.3. Wounded tissue recognition by microparticles coated with anti-actin antibodies

These results suggest that actin represents a potential wound-specific target that can be used for materials delivery to injured

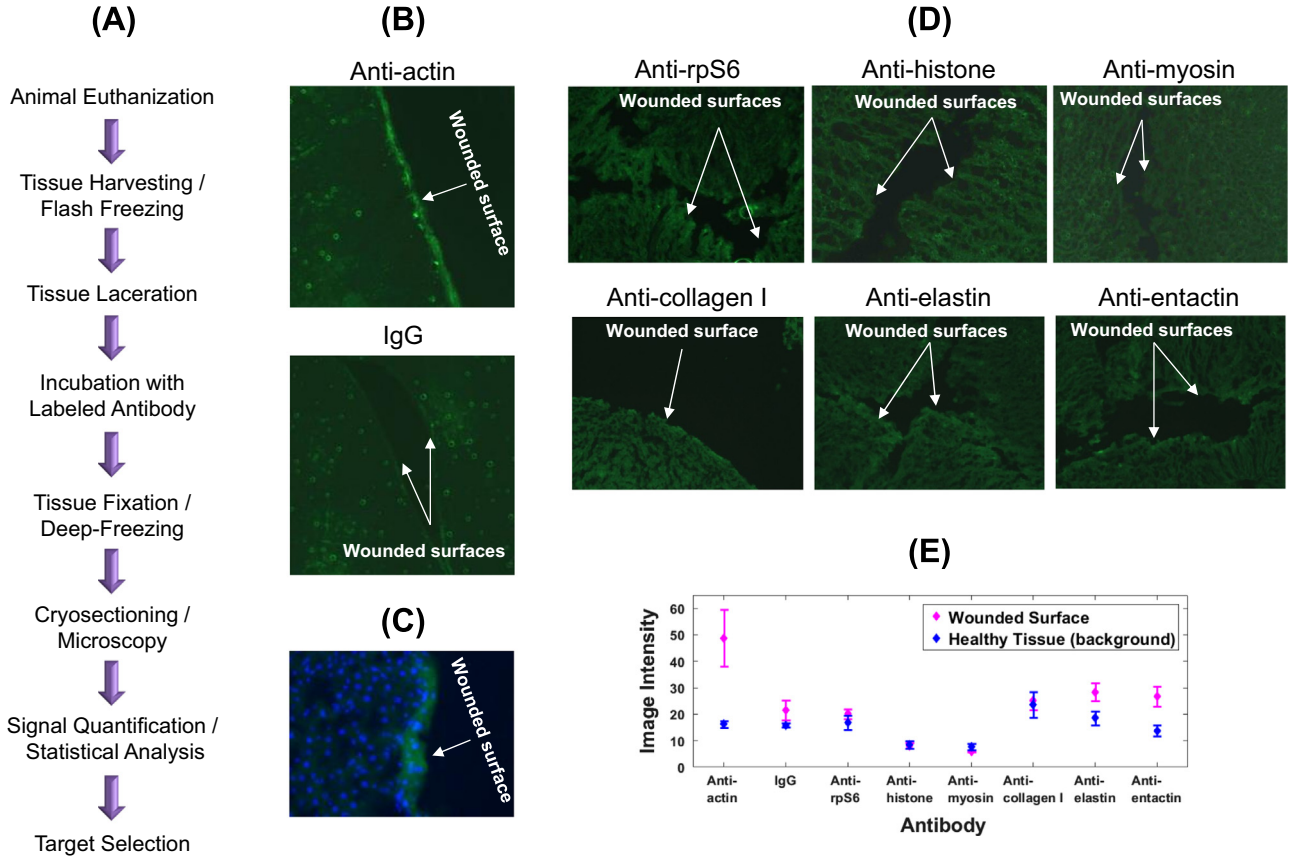


**Fig. 1.** Identification of actin as a wound-specific marker. (A). Outline of the experimental procedure for identification of protein targets exposed in injured tissue sites. Tissue samples are removed from the animal upon euthanization and lacerated under controlled conditions. Tissue samples are incubated with labeled (fluorescein) antibodies against the candidate target epitopes or with labeled non-specific antibodies (IgG) as negative controls. Tissue samples are then fixed, subjected to fast freezing and cryosectioning, and examined using fluorescence imaging microscopy. Microscopy images are captured and analyzed to assess whether the target epitopes were exposed in injured tissue areas as a means of their specific interaction with their cognate labeled antibodies. (B). Traumatized rat liver tissue treated with fluoresceinated (FITC-labeled) antibody against actin (top panel) or IgG (bottom panel). Images are representative of a series of horizontal slices across a vertical injury. Pictures were taken using inverted microscopy at 10 × magnification. (C). Fluorescence image of tissue sample treated with FITC-labeled anti-actin (green) and fluorescent nuclear counterstain, DAPI (blue). (D). Screening against intracellular (top panels) or extracellular matrix (bottom panels) proteins for specific wound exposure. (E). Quantitative analysis (mean and standard deviation) of image intensities at the wounded surface *versus* the neighboring healthy tissue areas for the wound targets tested.

tissue sites. To provide experimental feasibility for this assumption, we assessed transport and wound-specific binding of polystyrene beads as surrogate carrier particles conjugated to antibodies recognizing actin epitopes exposed in wounded tissues *ex vivo*. The results of these experiments showed that beads conjugated to anti-actin antibodies specifically bind to injured liver tissue (Fig. 4A).

Next, we evaluated transport and wound-specific binding of the aforementioned microparticles *in vivo* using an aggressive anesthetized bleeding animal model. In these experiments, polystyrene beads were tagged with either anti-actin antibodies (for wound targeting) or anti-IgG (negative control). Anesthetized rats were subjected to a grade IV lethal liver injury and allowed to bleed for a total of five minutes before the antibody-coated bead sample was applied to the wound in the presence of blood flow (see Materials and Methods section for experimental details). Following treatment, the animals were euthanized, and the liver harvested, washed, fixed and sectioned for fluorescence microscopy. The results (Fig. 4B) show specific targeting of the wound site *in vivo*, providing feasibility for use of actin as a target for specific delivery of materials to an aggressively bleeding wound site.

## 4. Discussion

In this study we describe an approach for identification of injury-specific protein markers that are rapidly exposed in wounded tissues and can be targeted for localized delivery of compounds of interest specifically at the affected area immediately upon trauma. Using this approach we discovered actin as such injury-specific marker. Wound-specific exposure of actin was verified in various animal tissues, suggesting the targetability of this protein independently of tissue type. We further showed that this marker is exposed in trauma areas within seconds upon tissue damage and remains stable over time and in the presence of blood. Importantly, by exploiting this protein as a wound-specific target, we selectively delivered microparticles conjugated to actin antibodies to injured areas in an *ex vivo model* of animal tissue trauma and an *in vivo* model of lethal animal injury. Given that tissue injury results in cell lysis and exposure of intracellular components normally not present on the cell surface, it is anticipated that the method described here for discovery of wound-specific epitopes, and the identification of actin as such marker, will be broadly applicable regardless of wound size and/or location.

Actin represents one of the most evolutionarily conserved and abundant intracellular eukaryotic proteins, providing a potentially high concentration of target epitopes for wound recognition. In addition, in its cytoskeletal form, actin is only partly soluble, a

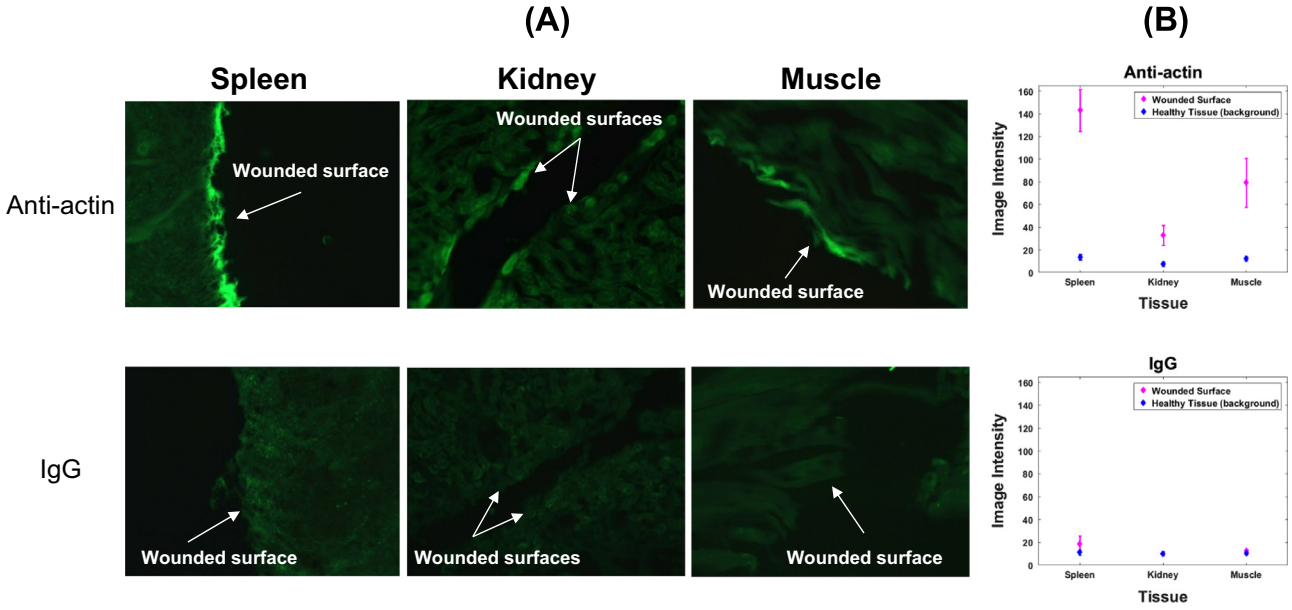


**Fig. 2.** Actin recognition in injured sites of various tissues. (A). Traumatized rat spleen (left), kidney (middle) or muscle (right) tissues were treated with fluoresceinated (FITC-labeled) antibody against actin (top panels) or IgG as negative control (bottom panels). (B). Quantitative analysis (mean and standard deviation) of image intensities at the wounded surface *versus* the neighboring healthy areas for spleen, kidney and muscle tissues treated with anti-actin (top panel) or IgG (bottom panel) antibodies.

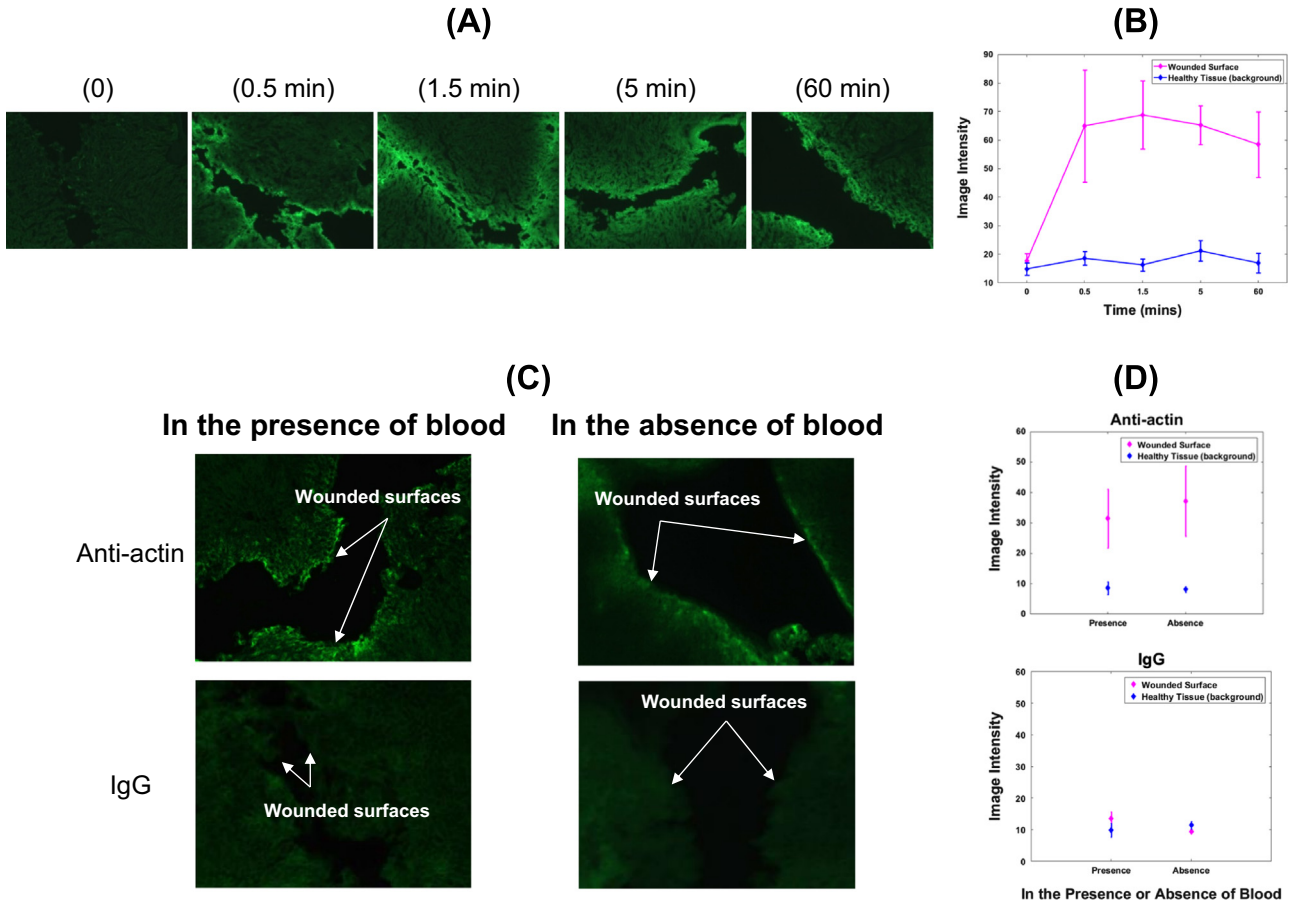


**Fig. 3.** Availability of actin epitope in wounded tissue. (A). Fluorescence images from experiments assessing wound-specific binding of FITC-labeled anti-actin antibodies upon incubation with injured rat liver *ex vivo* for various time periods. (B). Quantitative analysis (mean and standard deviation) of image intensities at the wounded surface *versus* the neighboring healthy tissue areas upon incubation of injured tissue samples with anti-actin antibody for various incubation times. (C). Targeting of actin in wounded rat liver tissue immersed in blood (left panels) or in the absence of blood (right panels). Excised wounded liver tissue in each case was treated with either FITC-labeled antibody against actin (top panels) or FITC-labeled IgG antibody as negative control (bottom panels). (D). Quantitative analysis of image intensities at the wounded surface *versus* the neighboring healthy tissue areas for tissue samples treated with anti-actin (top panel) or IgG (bottom panel) antibodies in the presence or absence of blood.

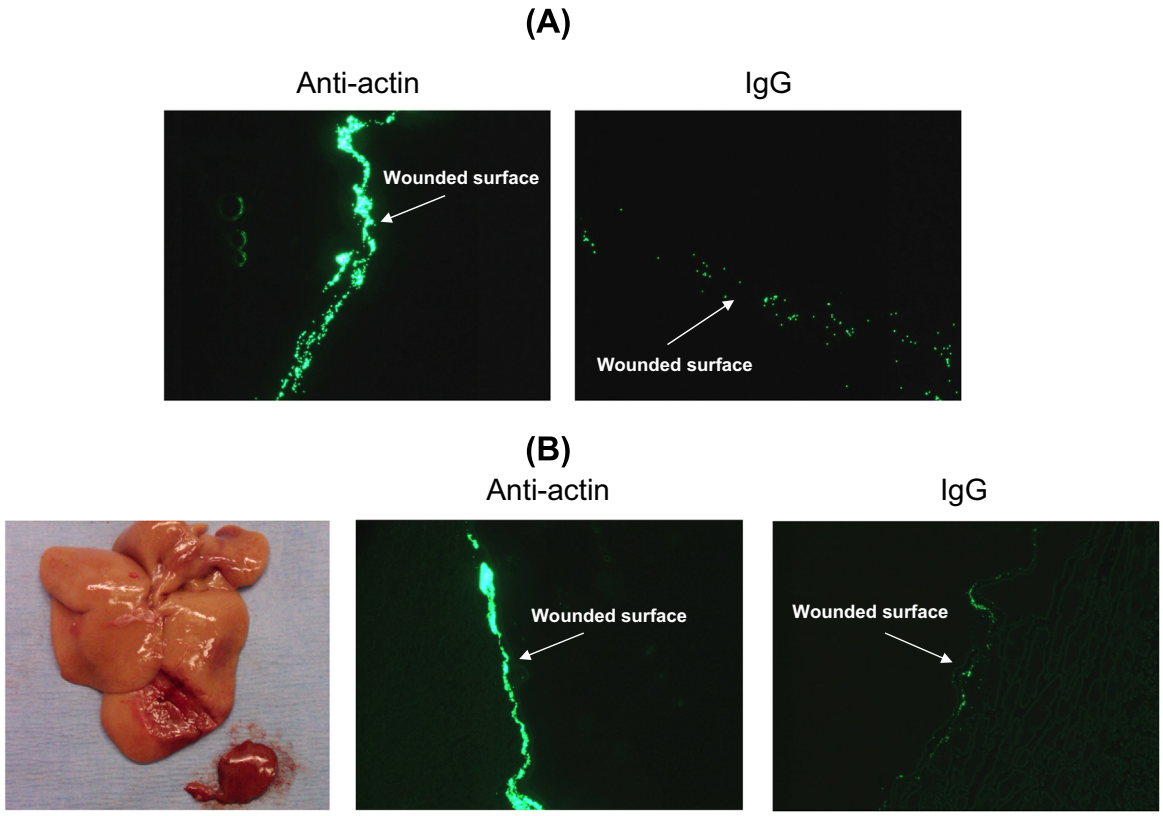


**Fig. 4.** Anti-actin-conjugated beads binding to wounded liver tissue *ex vivo* and *in vivo*. (A). Anti-actin-conjugated beads binding to injured liver tissue *ex vivo*. Excised liver tissue was incubated with labeled polystyrene beads conjugated to either anti-actin antibodies (left panel) or IgG as negative control (right panel). (B). Assessment of actin as a wound-specific biomarker *in vivo*. Transport and wound-specific binding was tested in a grade IV anesthetized rat lethal liver injury model. Lacerated liver tissue was incubated with labeled polystyrene beads conjugated to either anti-actin antibody or IgG (negative control). Following treatment, the anesthetized animals were euthanized, and the livers harvested, washed, fixed and sectioned for fluorescence microscopy. Left panel: Typical liver injury generated in this procedure. Middle panel: Beads tagged with anti-actin antibodies. Right panel: Beads tagged with IgG.

property that prolongs its presence at the injured site even under significant blood flow. This attribute of actin was evident in our study through its targetability under conditions of aggressive bleeding *in vivo*. In accordance with these results, it was recently found that cell death does not lead to complete loss of cytoskeleton structural integrity; instead damaged cells retain polymerized actin filaments that upon exposure serve as a signal to initiate a controlled immune response toward tissue repair [2]. Another significant attribute of actin as a wound target is that its presence at the injured site does not require *de novo* synthesis; this protein is present intracellularly (thus not available for binding in healthy tissue) but becomes exposed upon cell lysis caused by injury. Accordingly, the availability of this wound-specific target is expected to be rapid upon trauma. In agreement with this hypothesis, our experiments suggested that binding of actin antibodies to injury-exposed actin occurs within 30 s.

Identification and subsequent utilization of wound-specific targets could have important applications. For example, it would allow target recognition moieties to be multivalently bound to the surface of small size particles (liposomes, nanoparticles, or other type carriers), thus allowing targeted delivery of therapeutic loads to virtually any wound area regardless of geometry and intracavitary location. Targeted delivery to injured sites can minimize the amount of therapeutic agents and materials that must be delivered to a wound area, improve the specificity of delivery to the critical site of tissue damage, and minimize potential collateral damage to the surrounding healthy tissue. In this regard, it is envisioned that wound-specific targets can be utilized in the clinic to enable targeted delivery of agents that attenuate blood loss caused by penetrating wounds or surgical trauma to the skin or internal organs. Wound-targeting systems can be administered directly to the injured site, such as by irrigation of the wound with a solution containing a particular composition, or systemically, such as by intravenous delivery, upon optimization for increased circulatory life-time and reduced clearance by the immune system.

Wound targeting moieties can include polyclonal, monoclonal, chimeric and humanized antibodies (or antigen-binding fragment regions) or peptides with affinity for one or more epitopes within the specific protein target of interest. Those targeting moieties can be conjugated on the surface of nano- or microparticles using a variety of techniques, including covalent conjugation to polyethylene glycol (PEG) strands at the surface of the particles [11] or use of biotinylated [15], amine-reactive [3,18,23,24] and thiol-reactive copolymers [12,19] that permit protein chemical conjugation under non-denaturing conditions [6,14]. Types of carriers may include, for example, liposomes or various types of nanoparticles [1,4,7,17,21], microspheres [8], nanospheres [5], micelles [9,20], and dendrimers [25]. In support, our preliminary results have demonstrated successful wound-specific recognition of injured rat liver tissue by liposome particles conjugated to anti-actin antibodies and carrying encapsulated peptide payloads (to be described elsewhere).

In conclusion, we have identified actin as an injury-specific protein marker that gets exposed at the wounded site upon cell damage. The identification of actin as a wound-specific target suggests that abundant proteins with housekeeping functions can be explored as potential targets for specific delivery of therapeutic materials to injured sites. Identification of damaged tissue-specific

biomarkers has the potential for fundamentally impacting human care and trauma patient outcomes.

## Conflict-of-interest statement

The authors declare financial interests. Parts of this study are included in US patent Number 8,663,932 (Dresios and Griffey, “Methods and compositions for wound treatment”).

## Acknowledgements

We thank Scott D. Stewart and Dr. Gary A. Jongeward for critical reading of the manuscript and useful insights. We thank Zemmie Pollock (Lovelace Respiratory Research Institute) for providing technical expertise on animal experiments. This work was supported by funding from the Defense Advanced Research Projects Agency (W911NF-10-C-0065). The views expressed are those of the authors and do not reflect the official policy or position of the Department of Defense or the U. S. Government.

## Appendix A. Supporting information

Supplementary data associated with this article can be found in the online version at http://dx.doi.org/10.1016/j.bbrep.2016.05.013.

## References

[1] S.A. Agnihotri, N.N. Mallikarjuna, T.M. Aminabhavi, Recent advances on chitosan-based micro- and nanoparticles in drug delivery, J. Control. Release 100 (2004) 5–28.
[2] S. Ahrens, S. Zelenay, D. Sancho, P. Hanč, S. Kjær, et al., F-actin is an evolutionarily conserved damage-associated molecular pattern recognized by DNGR-1, a receptor for dead cells, Immunity 36 (2012) 635–645.
[3] K. Emoto, Y. Nagasaki, M. Iijima, M. Kato, K. Kataoka, Preparation of non-fouling surface through the coating with core-polymerized block copolymer micelles having aldehyde-ended PEG shell, Colloids Surf. B: Biointerfaces 18 (2000) 337–346.
[4] M.M. Gasper, D. Blanco, M.E. Cruz, M.J. Alonso, Formulation of L-asparaginase-loaded poly(lactide-co-glycolide) nanoparticles: influence of polymer properties on enzyme loading, activity and *in vitro* release, J. Control. Release 52 (1998) 53–62.
[5] R. Gref, Y. Minamitake, M.T. Peracchia, V. Trubetskoy, V. Torchilin, R. Langer, Biodegradable long-circulating polymeric nanospheres, Science 263 (1994) 1600–1603.
[6] J. Huwyler, D. Wu, W.M. Pardridge, Brain drug delivery of small molecules using immunoliposomes, Proc. Natl. Acad. Sci. USA 93 (1996) 14164–14169.
[7] F.B. Landry, D.V. Bazile, G. Spenlehauer, M. Veillard, J. Kreuter, Degradation of poly(D,L-lactic acid) nanoparticles coated with albumin in model digestive fluids (USP XXII), Biomaterials 17 (1996) 715–723.
[8] J.K. Li, N. Wang, X.S. Wu, A novel biodegradable system based on gelatin nanoparticles and poly(lactic-co-glycolic acid) microspheres for protein and peptide drug delivery, J. Pharm. Sci. 86 (1997) 891–895.
[9] A.,N. Lukyanov, V.P. Torchilin, Micelles from lipid derivatives of water-soluble polymers as delivery systems for poorly soluble drugs, Adv. Drug. Deliv. Rev. 56 (2004) 1273–1289.
[10] J.E. Mogford, G.E. Davis, S.H. Platts, G.A. Meininger, Vascular smooth muscle alpha v beta 3 integrin mediates arteriolar vasodilation in response to RGD peptides, Circ. Res. 79 (1996) 821–826.
[11] J.C. Olivier, Drug transport to brain with targeted nanoparticles, NeuroRx 2 (2005) 108–119.
[12] J.C. Olivier, R. Huertas, H.J. Lee, F. Calon, W.M. Pardridge, Synthesis of pegylated immunonanoparticles, Pharm. Res. 19 (2002) 1137–1143.
[13] C. Otten, P.F. van der Ven, I. Lewrenz, S. Paul, A. Steinhagen, et al., Xirp proteins mark injured skeletal muscle in zebrafish, PLoS ONE 7 (2) (2012) e31041, http://dx.doi.org/10.1371/journal.pone.0031041.
[14] M.J. Roberts, M.D. Bentley, J.M. Harris, Chemistry for peptide and protein PEGylation, Adv. Drug. Deliv. Rev. 54 (2002) 459–476.
[15] A.K. Salem, S.M. Cannizzaro, Davies, et al., Synthesis and characterisation of a degradable poly(lactic acid)-poly(ethylene glycol) copolymer with biotinylated end groups, Biomacromolecules (2001) 575–580.
[16] D. Sancho, O.P. Joffre, A.M. Keller, N.C. Rogers, D. Martínez, et al., Identification of a dendritic cell receptor that couples sensing of necrosis to immunity, Nature 458 (2009) 899–903.
[17] K.S. Soppimath, T.M. Aminabhavi, A.R. Kulkarni, W.E. Rudzinski, Biodegradable polymeric nanoparticles as drug delivery devices, J. Control. Release 70 (2001) 1–20.
[18] J. Tessmar, A. Mikos, A. Gopferich, Amine-reactive biodegradable diblock copolymers, Biomacromolecules 3 (2002) 194–200.
[19] J. Tessmar, A. Mikos, A. Gopferich, The use of poly(ethylene glycol)-block-poly (lactic acid) derived copolymers for the rapid creation of biomimetic surfaces, Biomaterials (2003) 4475–4486.
[20] V.P. Torchilin, Drug targeting, Eur. J. Pharm. Sci. 11 (Suppl. 2) (2000) S81–S91.
[21] N. Wang, X.S. Wu, J.K. Li, A heterogeneously structured composite based on poly(lactic-co-glycolic acid) microspheres and poly(vinyl alcohol) hydrogel nanoparticles for long-term protein drug delivery, Pharm. Res. 16 (1999) 1430–1435.
[22] N.T. Wright, J.D. Humphrey, Denaturation of collagen via heating: an irreversible rate process, Annu. Rev. Biomed. Eng. 4 (2002) 109–128.
[23] Y. Yamamoto, Y. Nagasaki, M. Kato, K. Kataoka, Surface charge modulation of poly(ethylene glycol)poly(L-lactide) block copolymer micelles: conjugation of charged peptides, Colloids Surf. B: Biointerfaces 16 (1999) 135–146.
[24] Y. Yamamoto, Y. Nagasaki, Y. Kato, Y. Sugiyama, K. Kataoka, Long-circulating poly(ethylene glycol)-poly(-lactide) block copolymer micelles with modulated surface charge, J. Control. Release 77 (2001) 27–38.
[25] H. Yang, S.T. Lopina, In vitro enzymatic stability of dendritic peptides, J. Biomed. Mater. Res. 76 (2006) 398–407.